JOURNAL OF APPLIED ELECTROCHEMISTRY **23** (1993) 1244–1250

Hydrated structures in the anodic layer formed on lead electrodes in H_2SO_4 solution

B. MONAHOV, D. PAVLOV

Central Laboratory of Electrochemical Power Sources, Bulgarian Academy of Sciences, 1113 Sofia, Bulgaria

Received 2 November 1992; revised 23 February 1993

SEM and TEM observations of the corrosion layer obtained during the potentiostatic oxidation of lead electrodes in H_2SO_4 solution have shown that, at potentials above 1.00 V vs Hg/Hg_2SO_4, a lead dioxide layer is formed with crystal and gel-like (hydrated) structures. The crystal zones of the corrosion layer contain α- and β-PbO_2 crystals. Applying controlled thermal degradation it has been established that hydrated zones (denoted as $PbO(OH)_2$) comprise about 10% of the corrosion layer. For comparison, the lead dioxide active mass of the lead-acid battery is hydrated over 30%. On prolonged polarization of the lead dioxide electrode at 1.50 V, the basic electrochemical reaction that takes place is oxygen evolution. It has been suggested that this reaction occurs mainly at the interface crystal/gel-like zones. On opening the circuit, the electrode potential reaches the equilibrium potential for the $PbO_2/PbSO_4$ system within a rather long period. This potential decay is related to the diffusion of oxygen through the bulk of the corrosion layer (probably through its hydrated zones) to the solution and to the metal. A suggestion is made that hydrated zones are also involved in the oxygen reaction.

1. Introduction

The phase composition of the anodic layer formed on lead electrodes in sulphuric acid solutions depends on the oxidation potential and the electricity that passes through the electrode. Depending on the potential, four electrode systems are formed: $Pb/PbSO_4$, $Pb/PbO/PbSO_4$, Pb/PbO_2 and $Pb/PbO/PbO_2$ [1–4]. In the potential region between −0.95 V and −0.45 V, a $PbSO_4$ crystal layer is formed on the electrode surface. From −0.45 V to +0.95 V, the characteristic diffraction lines for $PbSO_4$ and tet-PbO crystals are observed in the X-ray diffractograms. Above +0.95 V, the Pb/PbO_2 electrode system is formed [1–3]. During continuous anodic polarization at potentials higher than +1.20 V, a tet-PbO sublayer is detected between the lead dioxide layer and the metal surface [4]. The X-ray diffractograms however reflect only the crystalline phases. But the corrosion layer may also contain amorphous zones.

The positive lead dioxide active material (PAM) of lead–acid batteries is formed by electrochemical oxidation of basic lead sulphates and lead oxide. Until recently PAM was considered to be a crystalline system. It has been established, however, that it contains amorphous hydrated phases as well [5, 6]. Based on these considerations, a new concept has been proposed which views the structure of PAM as a gel-crystal system with electronic and proton conductivity [7].

The question arises whether the anodic layer formed in the PbO_2 potential region does not also contain amorphous hydrated phases and, if so, what is their amount? What is the influence of the hydrated zones on the electrochemical processes? The aim of the present paper is to answer these questions.

2. Experimental details

Flat electrodes sized 17 mm × 11 mm × 1 mm and made of lead (99.99%) were used. The electrolyte in all experiments was a 0.5 M H_2SO_4 solution. A platinum plate was used as a counter electrode and the reference electrode was Hg/Hg_2SO_4 in the same solution. The electrodes were polarized at constant potential for 16 h. The X-ray diffractograms (Kα, 10–70° (2Θ), 1° min^{-1}) of the anodic layer were recorded. Samples of the anodic layer were also subjected to SEM observations. Parts of the corrosion layer were scraped off the electrodes for transmission electron microscopic (TEM) analysis. To determine the water content in the corrosion layer, the latter was subjected to thermal decomposition at linear temperature sweeps.

3. Results

3.1. *Crystal morphology and structure of the anodic layer*

Figure 1 presents a SEM micrograph of the anodic layer obtained at −0.60 V.

The anodic layer consists of interconnected $PbSO_4$ crystals about 1 μm in size. There are only individual crystals of larger dimensions (about 10 μm) and a few others with irregular shape and sizes smaller than 1 μm.

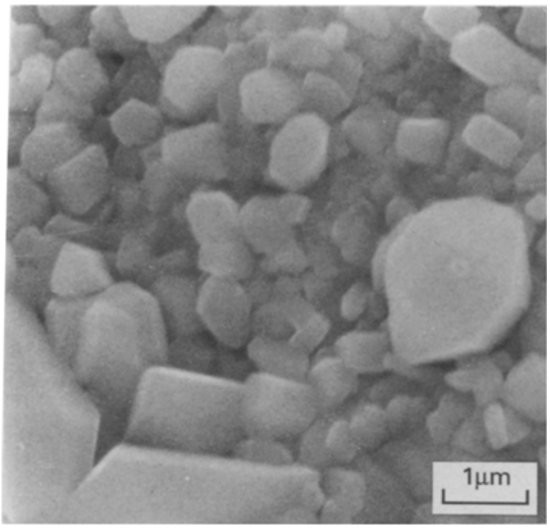

Fig. 1. SEM micrograph of the anodic layer obtained after 16 h of polarization at −0.60 V.

Figure 2(a) presents the structure of the layer; the morphology of the crystals of the anodic layer obtained at +0.90 V is shown in Fig. 2(b).

The anodic layer consists of submicron particles interconnected in a continuous mass with some cracks. As a result of recrystallization processes, large $PbSO_4$ crystals (10 μm) have grown on the surface of this layer.

The macrostructure of the anodic layers obtained at +1.00 V, +1.30 V and at +1.50 V is shown in Fig. 3 (a), (c) and (e), and the microstructure of the particles building up the layer is given in Fig. 3 (b), (d) and (f).

Lead dioxide covers the electrode surface as a continuous layer (fig. 3 (a), (c) and (e)). It can be seen at larger magnifications that this layer consists of interconnected grains or globules. Some of these form large agglomerates with well pronounced boundaries. This is most evident with the anodic layer formed at +1.30 V. The general conclusion can therefore be drawn that the lead dioxide layer formed potentiostatically at potentials over +1.00 V has a gel-like structure at its interface with the solution.

To determine the internal structure of the lead dioxide particles, pieces of the anodic layer (obtained after polarization for 16 h at 1.50 V) were observed by a transmission electron microscope. Two of the micrographs are shown in Fig. 4.

The particles of the anodic layer are not homogeneous in mass density. Dark zones have high material density and, according to the electron diffraction analysis, they are crystalline in structure. Other zones are transparent for the electron beam and have no crystal structure. As established earlier [6] this is typical of hydrated zones. On comparing the TEM micrographs of the corrosion layer with those of the active material [6] it can be seen that the corrosion layer is far less hydrated than PAM. This is due to the different initial products from which lead dioxide is formed.

3.2. *Crystallinity of the anodic layer*

The phase composition of the anodic layer was determined by XRD analysis. The dependance of the relative intensity of the characteristic diffraction lines for the crystalline phases of the anodic layer on the potential is presented in Fig. 5. The curves obtained are analogous to those reported in [1].

Figure 5(a) shows that, after the electrode surface is covered by a layer of $PbSO_4$, these crystals grow slightly with increasing potential up to +0.95 V. As established earlier [8, 9] the $PbSO_4$ crystals formed create a semipermeable membrane which inhibits the transport of SO_4^{2-} ions along the pores and, hence, the solution in the pores is alkalized.

The conversion of the $PbSO_4$ layer into a membrane facilitates the formation of a tet-PbO layer between the metal and the $PbSO_4$ layer. Fig. 5(b) shows that the thickness of this layer grows with increasing potential up to +1.40 V. Tet-PbO has a predominant orientation along the [110] plane corresponding to the diffraction line at 2.81 Å. Up to 0 V, this orientation effect is weak, increasing considerably at higher potentials. Above +1.40 V, the line

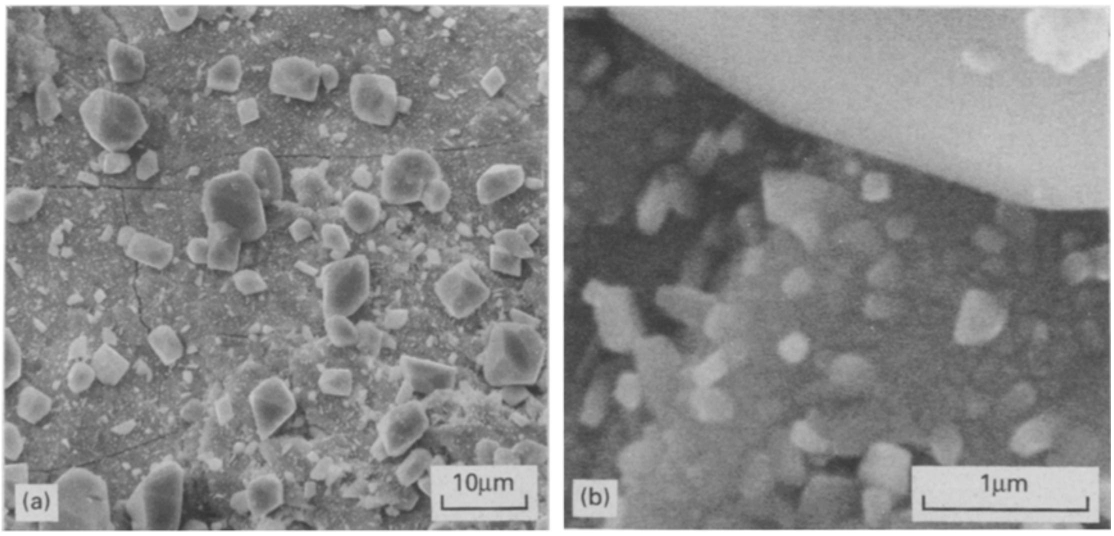

Fig. 2. SEM micrographs of the anodic layer obtained after 16 h of polarization at +0.90 V: (a) structure of the anodic layer; (b) crystal morphology.

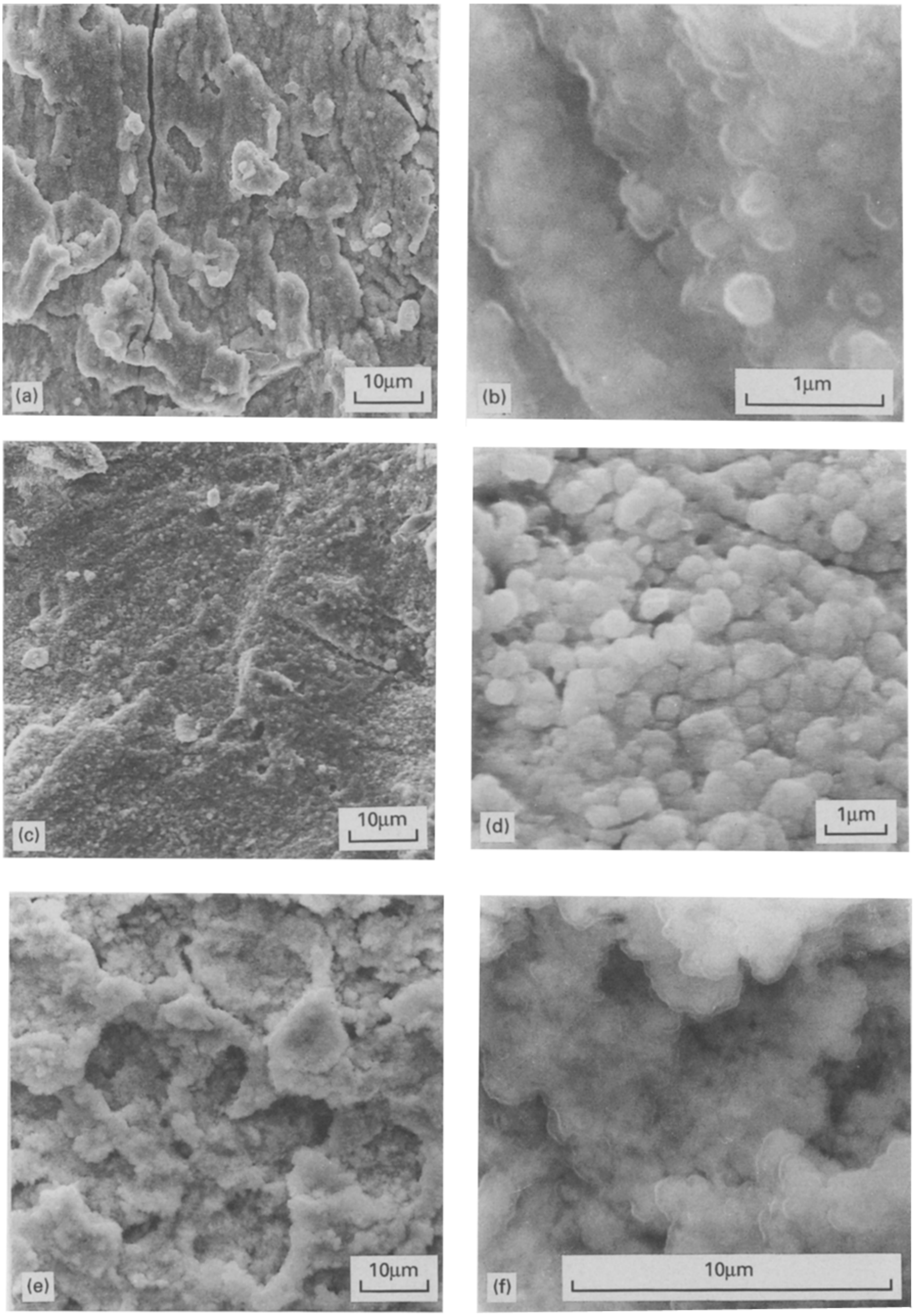

Fig. 3. SEM micrographs of the structure of the anodic layer (Fig. 3 (a), (c) and (e)), and of the morphology of its particles (Fig. 3 (b), (d) and (f)), obtained after 16 h of polarization at : (a) and (b) +1.00 V; (c) and (d) +1.30 V; (e) and (f) +1.50 V.

2.81 Å disappears from the diffractograms while the intensity of the 3.11 Å line is increased. The latter is characteristic for α-PbO_2. Figure 5(c) presents the relative intensities of the characteristic diffraction lines at $d = 3.80$ Å [1 1 0] for α-PbO_2 and $d = 3.50$ Å [1 1 0] for β-PbO_2. At potentials between +1.00 V and +1.20 V, β-PbO_2 predominates and only small amounts of α-PbO_2 are detected. β-PbO_2 is formed as a result of the oxidation of $PbSO_4$ crystals and α-PbO_2 to that of the tet-PbO layer. Figure 5 (b) and (c) shows that the oxidation of lead above +1.30 V is associated with the formation of α-PbO_2.

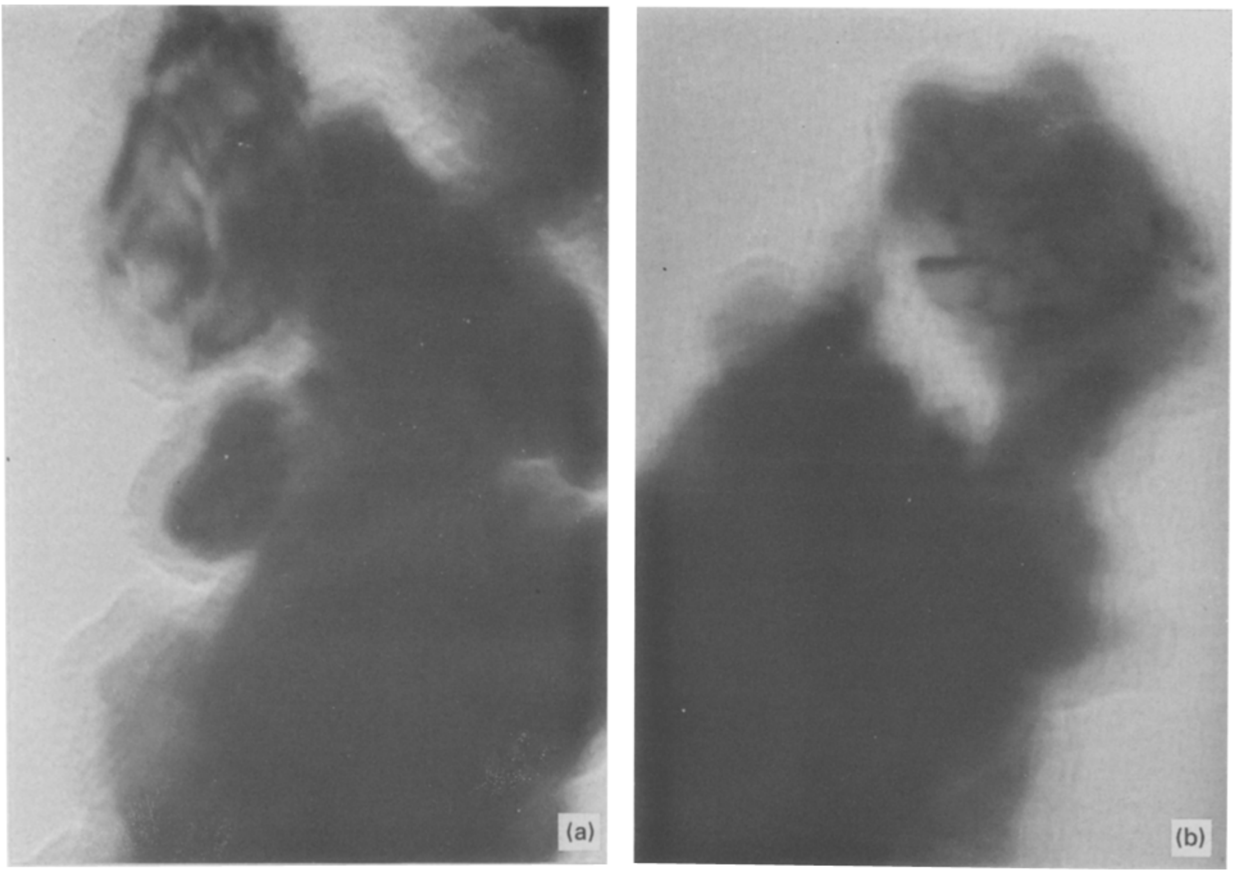

Fig. 4. TEM micrographs of particles of the anodic layer obtained on Pb electrodes polarized at 1.50 V for 16 h. Magnification: (a) TEM 100 000×, photograph 3×, total 300 000×; (b) TEM 200 000×, photograph 1×, total 200 000×.

Figure 5(d) presents the intensity curve for the line 2.48 Å for lead. From the changes in relative intensity of this line the dependence of the layer thickness on the oxidation potential can be determined. With increasing potential up to +0.95 V the thickness of the anodic layer also increases. After that it decreases considerably up to +1.30 V and increases again at higher potentials due to the formation of α-PbO_2.

It is known that the half-width of the X-ray diffraction lines depends on the average size of the crystals. The dependence between the half-width, B, of an XRD peak and the average crystal size, R, of the corresponding phase can be expressed, according to Scherrer [10] and Warren and Biscoe [11] by the following equation:

$$R = \frac{0.94Lg}{(B^2 - b^2)^{-1/2} \cos \Theta} \tag{1}$$

where L is the wavelength, Θ is the angle of the diffraction line under investigation, g is a geometric factor of the diffraction chamber, B is the measured half-width of the peak, and b is the half-width of the same line for a standard sample of the same material. Using the above equation, information can be obtained on the changes in crystal size of the $PbSO_4$, tet-PbO, α- and β-PbO_2 in the corrosion layer. These data are presented in Fig. 6.

The average size of the $PbSO_4$ crystals is 5–6 times greater than that of tet-PbO. With increasing potential from −0.60 V to +0.60 V, crystal sizes are changed slightly and increase at higher potentials (this can also be seen in Figs 1 and 2(a)). These larger crystals are formed as a result of recrystallization phenomena.

Tet-PbO crystals have lamellar habitus with smaller sizes along the [1 1 0] plane versus those along the [1 0 1] plane. These crystals, too, decrease in size with increasing potential.

The half-widths of lines 3.11 and 2.81 Å increase at potentials higher than 1.0 V. This may be due either to an abrupt decrease in crystal size or to a coincidence of the lines for tet-PbO and α-PbO_2 ($d = 3.11$ Å), and for tet-PbO and β-PbO_2 ($d = 2.81$ Å). The lines for the corresponding phases are slightly shifted from one another (by 0.02 Å only), but this is enough to give greater half-widths of the lines. Hence, the data about the crystal sizes at potentials higher than 1.00 V, given in Fig. 6, should be interpreted with some reservations. The actual dimensions of α-PbO_2 crystals are slightly larger, but it is difficult to assess exactly how much. This is much easier with β-PbO_2, where the size of the crystal zones along the (110) plane may be assessed from the half-width of the line with $d = 3.50$ Å (Fig. 6(d)).

From the SEM and TEM pictures it can be concluded that these are crystal zones in an amorphous mass. If the time of oxidation at +1.50 V is prolonged from 16 to 170 h, the half-widths of the lines for α-PbO_2 and β-PbO_2 (expressed by 2Θ) decrease from 1.45° and 1.15° to 0.95 and 0.65°, respectively. Probably recrystallization of part of the PbO_2 crystals occurs during this long period of oxidation and they grow in size.

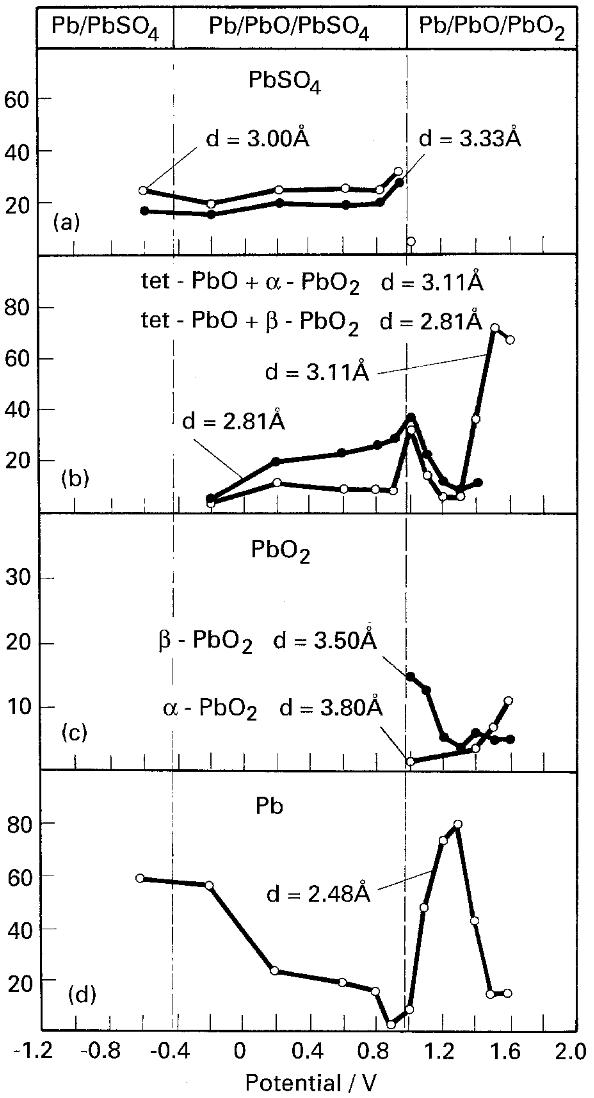

Fig. 5. Relative intensities of the characteristic X-ray diffraction lines of anodic layers obtained on Pb electrodes polarized for 16 h at different potentials.

3.3. *Water content in the corrosion layer*

It was necessary to find a direct proof of the presence of bonded water in the corrosion layer. This was achieved by controlled thermodegradation of the anodic layer [12]. A sample of the corrosion layer was put in a closed quartz tube and placed in an oven for controlled heating. The temperature was increased linearly up to 700° C at a rate of 25° C min^{-1}. Helium was blown through the apparatus at a flow rate of 60 ml min^{-1}. The oxygen and water evolved during the thermal decomposition of the corrosion layer were transported by the helium carrier gas and passed through a thermoconductivity detector (TCD) that registered the sum of H_2O and O_2 evolved. Then the gas mixture passed through a cold trap (with liquid nitrogen temperature). The thus dried gas mixture was admitted to a second TCD for measuring the amount of oxygen. The total quantity of water evolved was determined at the end of the experiment by evaporating the ice (water) from the cold trap through heating.

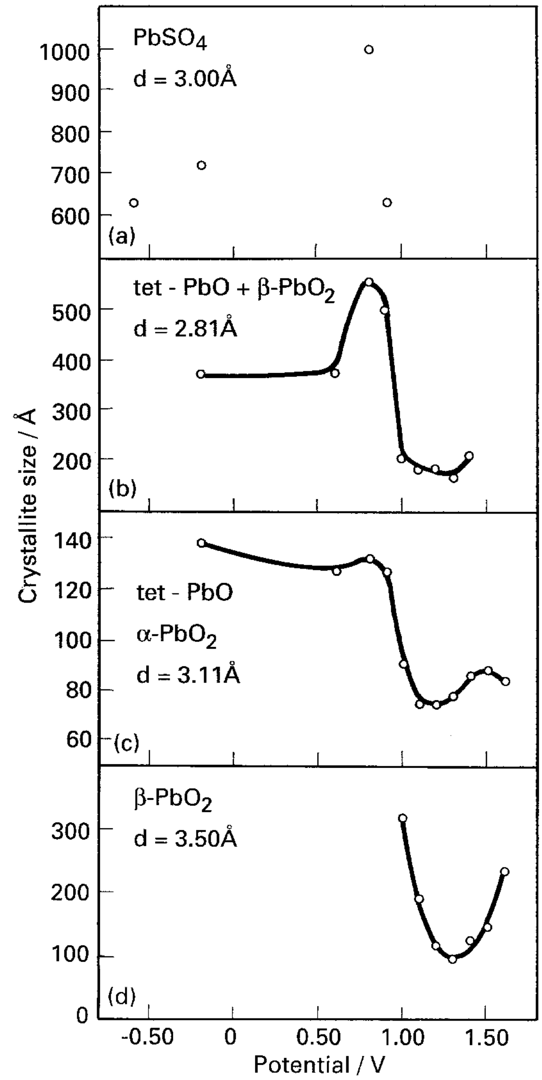

Fig. 6. Dependence of the average size of the crystals building up the anodic layer on the potential of oxidation.

The water content in the corrosion layers obtained at +0.90 V (80 h of oxidation), +1.30 V (80 h of oxidation) and +1.55 V (170 h of oxidation) was determined. The thermograms for these samples are shown in Fig. 7.

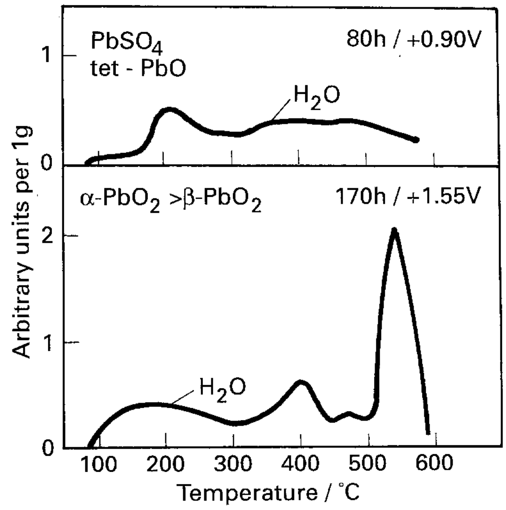

Fig. 7. Thermograms of water evolution from the anodic layer during controlled heating at 25° C min^{-1}.

Table 1.

Oxidation potential/ V	*$H_2O/(mm)^3g^{-1}$*
+0.90	1.40
+1.30	5.20
+1.55	7.90

During oxidation of tet-PbO (+0.90 V) water evolution starts at 200° C. The corrosion layer obtained at +1.55 V begins to evolve water at 100° C. Three maxima are observed on the thermogram. The third of them, at 500° C, is the most pronounced. This indicates that water is tightly bound to PbO_2.

Table 1 presents data on the amounts of water evolved by all three corrosion layers.

The corrosion layer obtained at +1.55 V consists mainly of lead dioxide. 438.8×10^{-6} M H_2O are contained in 7.9 mm^3 of the sample. One gram of PbO_2 contains 4184.1×10^{-6} M PbO_2. On comparing these two figures it becomes evident that only about 10.5% of the corrosion layer is hydrated or may have a gel-like structure.

3.4. *Oxygen evolution in the corrosion layer*

It may be expected that oxygen evolution will proceed at both the interface hydrated/crystal zones in the bulk of the corrosion layer and at the PbO_2 crystal/solution interface [7, 13]. As this is the potential limiting reaction during the 16 h polarization period, the potential behaviour immediately after opening the circuit is determined by the oxygen content in the corrosion layer. A Pb electrode was polarized at +1.60 V for 16 h and then the circuit was opened. The transient obtained is given in Fig. 8.

On opening the circuit, the electrode potential decreased to the equilibrium potential of the $PbSO_4$/PbO_2 system within about 16 min. This is a rather long period and can be related to the diffusion of oxygen from the bulk of the corrosion layer towards the solution. This is an indication that oxygen is evolved predominantly in the bulk of the corrosion layer. A high oxygen content in the corrosion layer has been reported earlier by Ruetschi *et al.* [14] and Kabanov *et al.* [15].

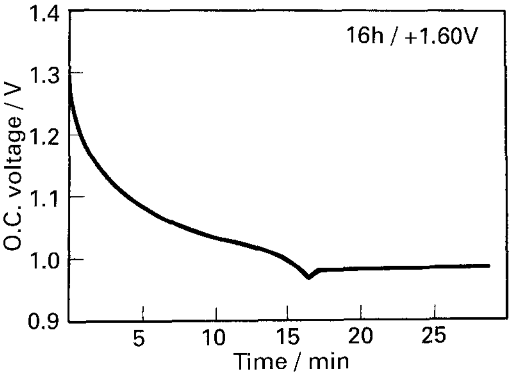

Fig. 8. Open circuit potential decay curves after polarization for 16 h at +1.60 V.

4. Discussion

During polarization of lead electrodes in H_2SO_4 solution at potentials up to +0.90 V vs Hg/Hg_2SO_4, Pb^{2+} ions are formed. These react with SO_4^{2-} and HSO_4^- ions from the solution forming $PbSO_4$. The latter's solubility in 0.5 M H_2SO_4 is 5 mg dm^{-3}. The solubility product is reached rapidly and a crystalline layer of $PbSO_4$ is deposited on the electrode surface (Fig. 1). Because of the impeded transport of SO_4^{2-} and HSO_4^- along the pores between the $PbSO_4$ crystals, the solution in them is alkalized. This creates thermodynamic conditions for the formation of tet-PbO between the $PbSO_4$ layer and the lead surface (Fig. 5). Oxidation of the metal proceeds further via transport of oxygen vacancies through the tet-PbO layer and of hydrogen ions and H_2O through the pores of the $PbSO_4$ membrane [3]. As a result of this oxidation, thin tet-PbO crystals are formed oriented along the [1 1 0] plane (Fig. 5(b) and (c)).

When a potential higher than +1.0 V is applied, Pb^{4+} ions are formed on the electrode surface. These are unstable in water solutions and form $Pb(OH)_4$.

$$Pb^{4+} + 4H_2O \longrightarrow Pb(OH)_4 + 4H^+ \qquad (2)$$

The $Pb(OH)_4$ is dehydrated partially or completely according to the following equations:

$$Pb(OH)_4 \longrightarrow PbO(OH)_2 + H_2O \qquad (3)$$

$$PbO(OH)_2 \longrightarrow PbO_2 + H_2O \qquad (4)$$

The metal surface is covered by a layer of PbO_2, $PbO(OH)_2$ and $Pb(OH)_4$, which layer has gel-like properties (Figs 3 and 4). The dehydration of the anodic layer reaches a steady state with time.

On electrode polarization in the potential region above +1.20 V, oxygen is evolved on the lead dioxide layer. Part of it diffuses through the anodic layer and reaches the metal surface causing its oxidation. α-PbO_2 is formed as a result of solid-state reactions (Figs 5 and 6). This is a process during which Pb is oxidized to α-PbO_2 after the electrode surface is covered by a PbO_2 layer with hydrated zones.

The hydrated zones, denoted as $PbO(OH)_2$, probably play a role in the process of oxygen evolution. The water they contain is incorporated in the electrode structure and the following reaction can readily proceed at the interface crystal/gel-like zones:

$$PbO(OH)_2 \longrightarrow PbO_2 + 2e^- + 2H^+ + O \qquad (5)$$

Oxygen atoms have a radius of 0.66 Å and can diffuse both to the solution and to the metal surface. The slow potential decay on opening the circuit is an indication of this process (Fig. 8). The electrons from Reaction 5 pass through the crystal zones of PbO_2 reaching the metal. Protons diffuse through the hydrated zones to the solution. In general, each of the above particles is strongly mobile, which enables the reaction to proceed in the bulk of the corrosion layer.

Hydrated lead dioxide is detected after 170 h of polarization (Table 1). This means that a certain steady phase composition is established in the anodic layer with a ratio between the hydrated and PbO_2 crystal phases approximately equal to 10%. To preserve this ratio unchanged, a hydration process must occur parallel to Reaction 5.

$$PbO_2 + H_2O \longrightarrow PbO(OH)_2 \qquad (6)$$

This means that water or OH^- ions get into the bulk of the corrosion layer causing part of it to be hydrated. This process may become a rate limiting one for this part of the oxygen reaction which proceeds in the bulk of the corrosion layer. Reactions 5 and 6 are associated with hydration and dehydration of PbO_2. These processes are in dynamic equilibrium and may result in recrystallization of PbO_2. The part of the oxygen reaction that proceeds at the interface PbO_2 crystals/solution probably comprises another slow elementary process, e.g. electron transfer.

Based on the above mechanism of oxygen evolution it can be concluded that hydrated zones in the corrosion layer play a significant role in this reaction. These zones are presumably concentrated mainly in the outer sublayers of the corrosion layer that are in contact with the solution.

References

[1] D. Pavlov, C. N. Poulieff, K. Klaja and N. Iordanov, *J. Electrochem. Soc.* **116** (1969) 316.
[2] D. Pavlov and N. Iordanov, *ibid.* **117** (1970) 1103.
[3] D. Pavlov, *Electrochim. Acta* **23** (1978) 845.
[4] K. R. Bullock and M. A. Butler, *J. Electrochem. Soc.* **133** (1986) 1085.
[5] D. Pavlov, I. Balkanov and P. Rachev, *ibid.* **137** (1987) 2390.
[6] D. Pavlov and I. Balkanov, *ibid* **139** (1992) 1830.
[7] D. Pavlov, *ibid.* **139** (1992) 3075.
[8] D. Pavlov and R. Popova, *Electrochim. Acta* **15** (1970) 1483.
[9] P. Ruetschi, *J. Electrochem. Soc.* **120** (1973) 331.
[10] P. Scherrer, *Nachr. Ges. Wiss., Goettingen* **98** (1918).
[11] B. E. Warren and J. J. Biscoe, *J. Am. Ceram. Soc.* **21** (1938) 16.
[12] Y. Amenomiya and R. C. Cvetanovic, *J. Phys. Chem.* **67** (144) (1963) 2046, 2705.
[13] D Pavlov, I. Balkanov, T. Halachev and P. Rachev, *J. Electrochem. Soc.* **136** (1989) 3189.
[14] P. Ruetschi, J. Ackerman and R. Amlie, *ibid.* **107** (1960) 325.
[15] B. N. Kabanov, E. S. Weisberg, I. L. Romanova and E. V. Krivolapova, *Electrochim. Acta* **9** (1964) 1197.